Multimaterial preform coextrusion for robust chalcogenide optical fibers and tapers

Guangming Tao,[1] Soroush Shabahang,[1] Esmaeil-Hooman Banaei,[1,2] Joshua J. Kaufman,[1] and Ayman F. Abouraddy[1,*]

[1]*CREOL, The College of Optics & Photonics, University of Central Florida, Orlando, Florida 32816, USA*

[2]*Department of Electrical Engineering & Computer Science, University of Central Florida, Orlando, Florida 32816, USA*

**Corresponding author: raddy@creol.ucf.edu*

Received March 27, 2012; revised May 8, 2012; accepted May 8, 2012;
posted May 8, 2012 (Doc. ID 165565); published June 28, 2012

The development of robust infrared fibers is crucial for harnessing the capabilities of new mid-infrared lasers. We present a novel approach to the fabrication of chalcogenide glass fiber preforms: one-step multimaterial extrusion. The preform consists of a glass core and cladding surrounded by a built-in, thermally compatible, polymer jacket for mechanical support. Using this approach we extrude several preform structures and draw them into robust composite fibers. Furthermore, the polymer cladding allows us to produce robust tapers with submicrometer core diameter.

OCIS codes: 060.0060, 060.2290, 060.2390.

Chalcogenide (ChG) glass fibers continue to attract interest for mid-infrared beam delivery, imaging fiber bundles, and nonlinear optics [1]. Nevertheless, the fragility and difficulty of handling and processing of ChG fibers [2] have limited their widespread use. This limitation is inherent to the traditional pathways of producing ChG fibers, such as double-crucible fiber drawing [3] and drawing from a rod-in-tube preform. By inserting a rod into a tube, typically obtained by drilling [4], rotational casting [5], or extrusion [6,7], some defects are inevitably introduced at the fiber core/cladding interface. Thermal drawing of the fiber improves the interface, but some bubbles are potentially trapped along the fiber. The double-crucible approach obviates this drawback, but it is a more complex process that produces a limited range of structures. In both cases, ChG fibers are coated with a layer of low-temperature polymer for mechanical support that cannot be codrawn or costretched with the ChG and limits the fiber working temperature [8]. The use of higher-temperature polymers is prohibited by the low processing temperatures of ChGs.

In this letter, we report a new ChG preform fabrication approach, *one-step multimaterial coextrusion*, that produces composite ChG/polymer preforms that are then drawn into *robust* fibers. A billet consisting of thermally compatible thermoplastic polymer and ChG is extruded into a preform provided with a built-in polymer jacket. The polymer does *not* participate in the optical functionality of the fiber, which is dictated by the ChG alone. We also produce robust, high-index-contrast, submicrometer-core-diameter tapers suitable for nonlinear optical applications without removing the polymer.

Our extrusion system consists of a sleeve (diameter 30–46 mm) inside a tube furnace. A billet is heated in the sleeve to allow viscous flow and is then extruded by a piston through a circular die [diameter 6–20 mm; Fig. 1(a)]. The billet is kept at slightly higher than the softening temperature, and ≈500 lbs of force is applied to extrude the billet at ~0.3–0.7 mm/min. Extrusion under pressure allows the use of lower temperatures and higher viscosities compared to fiber drawing, thereby reducing glass crystallization.

ChG rods were prepared from commercial glass (AMI, Inc.) by melt quenching [9], and polymer rods were prepared by thin-film processing [10]. The glasses used are $G_1 : As_2Se_3$, $G_2 : As_2Se_{1.5}S_{1.5}$, and $G_3 : As_2S_3$, with measured indices 2.904, 2.743, and 2.472 at 1.55 μm, respectively; the polymers used are polyethersulfone (PES) and polyetherimide (PEI). The large index contrast between the ChGs was chosen to test the limits of the extrusion process and to produce the high-index-contrast nanotapers described below. As a first example, we extrude a ChG-core (G_1), polymer-jacket (PES) preform [Figs. 1(c) and 1(d)] using a nested billet consisting of a ChG rod (11 mm diameter, 60 mm length) in a polymer tube [46 mm outer diameter, 140 mm length; Fig. 1(b)]. We refer to this structure as GP. See [11], which describes extrusion of Bragg preforms using these two materials.

We next extrude a preform with a ChG cladding surrounding the ChG core. We use a vertically stacked billet

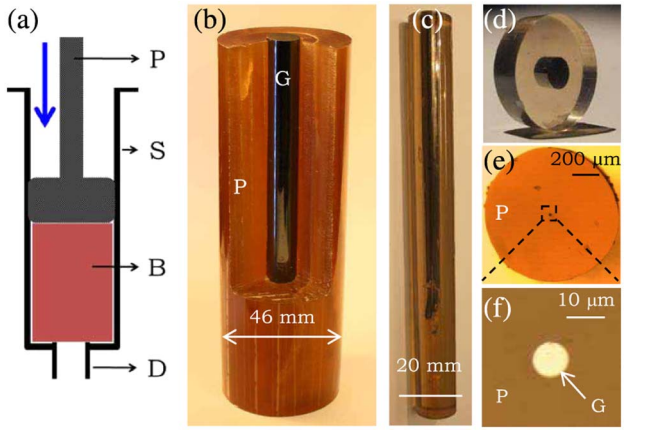

Fig. 1. (Color online) (a) Extrusion system. P, piston; S, sleeve; B, billet; D, die. (b) A hybrid polymer (P: PES) and ChG ($G : As_2Se_3$) billet. A section of the polymer was removed to reveal the structure. (c) Section of the extruded preform. (d) A disk (diameter 17.4 mm) cut from the extruded preform in (c). (e) Reflection optical micrograph of the fiber cross section and (f) the core.

comprising polished disks placed atop each other with the bottom (top) disk corresponding to the outermost (innermost) layer in the extruded preform [Fig. 2(a)]. The extruded preform consists of nested shells with the top-billet layer forming the core. We refer to this structure hereafter as GGP. The polymer protects the ChG from coming in contact with the die during extrusion or subsequently with the ambient environment. We do not observe any separation between the layers in the preforms (or in the subsequently drawn fibers). The larger thermal expansion coefficient of the polymer compared to the ChG eliminates in the preform the small gaps that inevitably exist at interfaces in the billet [12].

We draw each preform into a cane, and a 10-cm-long section of it is inserted into a polymer tube, which in turn is drawn into ≈100 m of continuous, robust, 1-mm-outer-diameter, 10-μm-core-diameter fiber [Fig. 2(b)]. Cross section of the GP fiber is shown in Figs. 1(e) and 1(f), and cross sections of two GGP fibers, G_1–G_3–PEI and G_2–G_3–PES, are shown in Figs. 2(c) and 2(d) and Figs. 2(e) and 2(f), respectively. The ChG in the latter two represents less than 0.1% of the fiber volume: 10 km of this fiber contains ~30 g of glass. The core-to-cladding diameter ratio here is ≈1/3. This ratio is controlled by changing the thicknesses of the disks in the billet and the pressure applied during extrusion. Reducing this ratio, however, reduces the yield of the useful preform length [13]. The built-in polymer jacket facilitates the fiber drawing compared to bare-glass-fiber drawing and helps avoid oxidation of the ChG. The fiber transmission losses (for a GGP fiber with As_2Se_3 core) evaluated by cutback measurements are ≈10.9 dB/m at 1.55 μm (using a laser diode) and ≈7.8 dB/m at 2 μm (using a Tm-doped fiber laser). The loss at the moment is limited by the purity of the glass.

The robustness of these composite ChG fibers is illustrated in Fig. 3. We measured the transmission over time (at 1.55 μm) after bending a GP fiber for 10 min intervals. There was no change for 1 in. bend diameters and larger, and we find no plastic memory in knots with diameters larger than 1 in. [Fig. 3(a)]. Results for a 0.5 in. bend

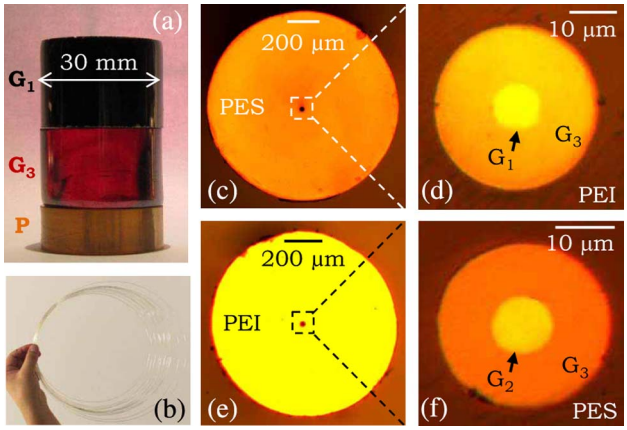

Fig. 2. (Color online) (a) Vertically stacked billet to produce a GGP preform. (b) Drawn GGP fiber. (c), (e) Transmission optical micrographs of the fiber cross sections, and (d), (f) reflection micrographs of the core. P, polymer; G_1 : As_2Se_3, G_2 : $As_2Se_{1.5}S_{1.5}$, and G_3 : As_2S_3.

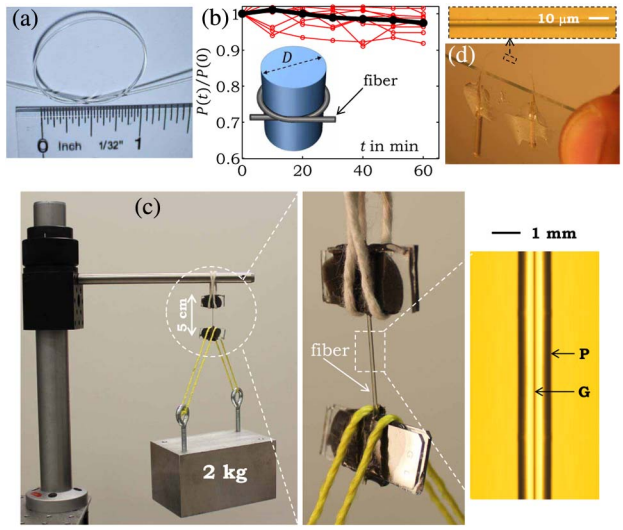

Fig. 3. (Color online) (a) A 1-mm-diameter fiber tied in a 1-in.-diameter knot. (b) Transmission over time for 10 fibers after bending the fiber with $D = 0.5$ in. bend diameter. The black curve is the average of all the measurements. (c) A 2 kg weight hanging from a 5-cm-long fiber. The inset shows the hanging mechanism. The fiber is attached to microscope slides using epoxy while keeping the ends free for optical measurements. (d) A robust multimaterial taper. The inset is a micrograph of the taper center.

diameter are plotted in Fig. 3(b). The transmission did not decrease after an hour by more than 10% (5% on average). We also investigated the effect of axial stress on optical transmission. We hang a 2 kg weight from multiple 5-cm-long GP fiber sections [Fig. 3(c)] for 18 h each and then measure the transmission (at 1.55 μm): it was unaffected in this experiment (compare to [2]). The fiber thus withstands 14.6 Kpsi (≈25.5 MPa) with *no change* in its performance over this extended period of time. This sets a lower limit on the fiber strength. Although the ChG diameter here is only 10 μm, the polymer jacket nevertheless allows for convenient handling and reduced ageing of the fibers. Therefore, the optical properties of the fiber are determined by the ChG, while the mechanical properties are determined by the polymer. Separating the functionalities in this way allows for them to be optimized independently.

A unique advantage of the thermally compatible built-in polymer jacket is in providing a mechanical scaffold for producing *robust* tapers without first removing the polymer. ChG nanotapers combine high optical nonlinearities with dispersion control but are hampered by their extreme fragility. The robustness of our multimaterial tapers is highlighted in Fig. 3(d), where we show a taper, produced using the system in [14,15], with core diameter 25 nm (outer diameter 3 μm).

We characterize GP and GGP tapers in three ways after cutting the taper at its center where the diameter is smallest ($d_{\min} = 1.4$ μm for the core in both tapers). (1) The *structure* is determined using scanning electron microscope (SEM) imaging, confirming that size reduction occurs at the same rate throughout the cross section during tapering [Figs. 4(a) and 4(d)]. (2) The *ChG-polymer interface* is determined by transmitting white light (coupled from the untapered end, $d_o = 10$ μm), since the polymer

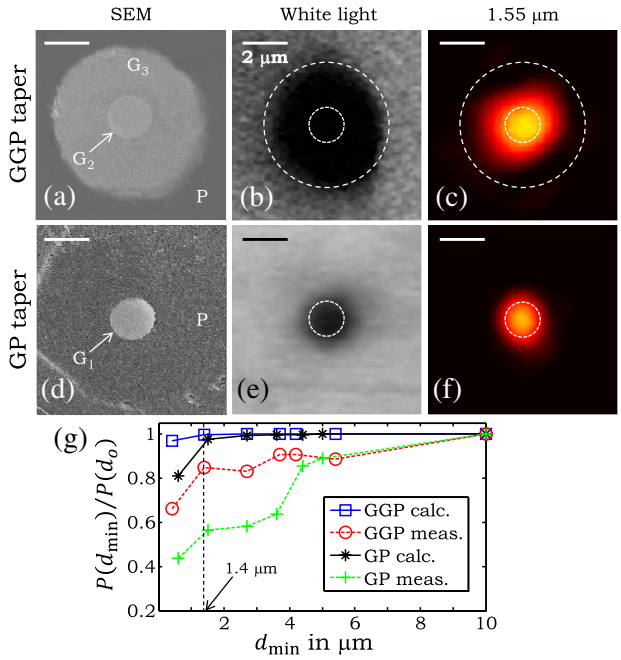

Fig. 4. (Color online) (a)–(c) Characterization of GGP and (d)–(f) GP tapers both having core $d_{\min} = 1.4\ \mu$m. (a), (d) SEM micrographs of the cross sections; (b), (e) white-light and (c), (f) 1.55 μm laser light near-field intensity images. Scale bars are 2 μm. Dashed white circles corresponding to the interfaces are guides for the eye. (g) Measured and calculated optical transmission at 1.55 μm for GGP and GP tapers with different $d_{\min}$ normalized with respect to the untapered fiber with $d_o = 10\ \mu$m. Dashed black line corresponds to $d_{\min} = 1.4\ \mu$m used in (a)–(f).

is transparent in the visible and the ChG is not [Figs. 4(b) and 4(e)]. (3) The *modal structure* is determined by transmitting 1.55 μm CW light (from a laser diode) through the core [Figs. 4(c) and 4(f)]. The mode is confined to the glass in the GGP taper owing to the high core/cladding index contrast (and extends into the polymer in the GP taper). We thus harness the mechanical strength of the polymer jacket without compromising the optical functionality of the taper.

We have measured the transmission in tapers of the same length (2.1 cm) with $d_{\min}$ from 10 μm down to 400 nm for GGP and GP tapers and compare the results in Fig. 4(g) to calculations performed using the scalar beam propagation method in OptiBPM 10.0 (Optiwave). The transverse simulation window was $50 \times 50\ \mu\text{m}^2$ and the step size was 0.1 μm in all three dimensions, with a perfectly matched layer boundary condition on all sides. We used the measured taper profile and realistic material losses (see [16]). The higher loss in the GP taper is due to absorption of the evanescent tail in the polymer, while in the GGP taper the light remains confined to the ChG. The measured losses are higher than the predictions. We attribute this to scatterers in the glass whose impact increases at smaller diameters, deformations in the cross section during tapering, and surface roughness at the interfaces (particularly for the GP taper).

In conclusion, we have described a novel one-step multimaterial preform extrusion process that produces hybrid ChG/polymer preforms that we draw into robust infrared fibers and tapers. The process helps obviate the mechanical limitations of ChG fibers and enables optimizing the optical properties for nonlinear applications.

We thank M. C. Richardson for assistance. This work was supported by the NSF (ECCS-1002295).

References

1. J. S. Sanghera, L. B. Shaw, and I. D. Aggarwal, IEEE J. Sel. Top. Quantum Electron. **15**, 114 (2009).
2. G. Delaizir, J.-S. Sangleboeuf, E. A. King, Y. Gueguen, X. H. Zhang, C. Boussard-Pledel, B. Bureau, and P. Lucas, J. Phys. D **42**, 095405 (2009).
3. R. Mossadegh, J. S. Sanghera, D. Schaafsma, B. J. Cole, V. Q. Nguyen, R. E. Miklos, and I. D. Aggarwal, J. Lightwave Technol. **16**, 214 (1998).
4. Z. Yang, T. Luo, S. Jiang, J. Geng, and P. Lucas, Opt. Lett. **35**, 3360 (2010).
5. B. Bureau, S. Maurugeon, F. Charpentier, J.-L. Adam, C. Boussard-Pládel, and X.-H. Zhang, Fiber Integr. Opt. **28**, 65 (2009).
6. D. Furniss and A. B. Seddon, J. Non-Cryst. Solids **256**, 232 (1999).
7. X. Feng, T. M. Monro, P. Petropoulos, V. Finazzi, and D. J. Richardson, Appl. Phys. Lett. **87**, 081110 (2005).
8. M. Saito, M. Takizawa, and M. Miyagi, J. Lightwave Technol. **6**, 233 (1988).
9. S. A. Ray Hilton, *Chalcogenide Glasses for Infrared Optics* (McGraw-Hill, 2009).
10. A. F. Abouraddy, M. Bayindir, G. Benoit, S. D. Hart, K. Kuriki, N. Orf, O. Shapira, F. Sorin, B. Temelkuran, and Y. Fink, Nat. Mater. **6**, 336 (2007).
11. D. J. Gibson and J. A. Harrington, J. Appl. Phys. **95**, 3895 (2004).
12. S. D. Savage, C. A. Miller, D. Furniss, and A. B. Seddon, J. Non-Cryst. Solids **354**, 3418 (2008).
13. A. B. Seddon, D. Furniss, and A. Motesharei, Proc. SPIE **3416**, 32 (1998).
14. S. Shabahang, J. J. Kaufman, D. S. Deng, and A. F. Abouraddy, Appl. Phys. Lett. **99**, 161909 (2011).
15. J. J. Kaufman, G. Tao, S. Shabahang, D. S. Deng, Y. Fink, and A. F. Abouraddy, Nano Lett. **11**, 4768 (2011).
16. Z. Ruff, D. Shemuly, X. Peng, O. Shapira, Z. Wang, and Y. Fink, Opt. Express **18**, 15697 (2010).